LA-UR-03-1414

Recent Research Developments in Atmospheric Sciences, accepted, 2003

Columnar Water Vapor Retrieval

Using Multi-Spectral Satellite Data

Petr Chylek[1] and Christoph C. Borel

Space and Remote Sensing Sciences
Los Alamos National Laboratory
Los Alamos, New Mexico 87545, USA

Short title: Water Vapor

ABSTRACT

We review several methods of columnar water vapor retrieval using satellite multispectral data. Error analysis suggests that the radiometric calibration error and an uncertainty in atmospheric aerosol loading are the largest sources of errors of the satellite based columnar water vapor retrieval using the near infrared wavelengths. During the nighttime the outgoing top of the atmosphere radiances in mid-infrared wavelengths region are more sensitive to changes in columnar water vapor amounts than the radiances at the long (10 to 12 μm) infrared wavelengths.

[1]Also associated with the Department of Physics, New Mexico State University, Las Cruces, New Mexico, USA, and with the Department of Physics and Atmospheric Science, Dalhousie University, Halifax, Nova Scotia, Canada.

Corresponding author: Petr Chylek, Space and Remote Sensing Sciences, Los Alamos National Laboratory, Mail Stop C323, Los Alamos, NM 87545; email:chylek@lanl.gov

1. INTRODUCTION

The total amount of water vapor in the atmosphere is an important parameter needed for the understanding and modeling of Earth's hydrological cycle and climate. Water vapor plays a major role in redistribution of water and energy within the global geophysical system. The annual average of columnar water vapor (CWV) in the atmosphere varies between 0.25 g/cm^2 in polar regions to over 5 g/cm^2 in tropics [1].

Several remote sensing techniques using the microwaves, reflected near infrared solar radiation or terrestrial infrared radiation within 10 to 12 μm atmospheric window have been developed and are being used for water vapor monitoring.

In this paper we focus on the columnar water vapor retrieval in the near infrared solar radiation region. Section 2 introduces the atmospheric properties in the near infrared region. The Department of Energy (DOE) Multispectral Thermal Imager (MTI) is described in section 3. Sections 4 to 7 present basic methods of CWV retrieval, an error analysis and sensitivity study with respect to calibration errors and uncertainties in atmospheric parameters. Comparison of satellite retrieved CWV with ground measurements is presented in section 8. Section 9 introduces problems connected to the nighttime CWV retrieval.

2. ATMOSPHERIC TRANSMISSION IN NEAR INFRARED

The near infrared part of solar spectrum has several features that make it suitable for the CWV retrieval. In the NIR region the solar radiation is still quite strong. The interference form other atmospheric gases is relatively weak. Between 890 and 990 nm (Fig. 1) there is a strong absorption band centered near 942 nm and two weaker absorption bands centered around 906 and 977 nm [2].

The near infrared solar radiation within water vapor absorption bands reflected by atmospheric aerosol and earth's surface back towards the satellite instrument carries information concerning the water vapor abundance along its path. This information needs to be de-coupled from the surface reflectance and aerosol amount and translated into columnar water vapor amount. The methods used to retrieve the CWV from the satellite data use at least two spectral channels, one in and another adjacent to water vapor absorption band. Other channels may be added to improve the sensitivity of the top of the atmosphere outgoing radiances to small or large amounts of water vapor, or to minimize errors due to aerosols and the spectral dependence of the surface reflectivity.

3. THE MULTISPECTRAL THERMAL IMAGER

Although we will discuss the methods of the CWV retrieval in general terms, demonstrations of the accuracy will be presented using the Department of Energy research satellite instrument, the Multispectral Thermal Imager (MTI). The MTI [3] has fifteen spectral bands in visible and infrared region. Spectral characteristics of individual bands are listed in Table 1. The MTI pixel size is 5 m x 5 m in the visible and 20 m x 20 m in the infrared region; its swath width is around 12 km. While the MTI is not suitable for global climate change studies, it is well suited for measurement of local and regional scale environmental variables. The near IR bands E, F, and G, centered at the wavelength of 874, 940 and 1016 nm with area based band widths of 25, 56 and 48 nm are used for CWV retrieval. The MTI's small pixel size eliminates most errors in retrieval due to unresolved sub-pixel size cloudiness. In addition to clear sky images, partially cloudy scenes can be used for retrieval as long as clouds or cloud shadows do not affect a considerable fraction of an image.

4. COLUMNAR WATER VAPOR RETRIEVAL METHODS

The basic principal of the CWV retrieval is to measure the top of the atmosphere outgoing radiances within, and outside water vapor absorption bands and to relate their ratio to the amount of water vapor along the path. This constitutes the differential absorption (DA) method [4]. Alternatively one can use one wide and one narrow channel [5] within water vapor absorption band (narrow and wide (NW) method). Additional channels may be added to account for spectral dependence of surface reflectivity. This has been done in methods known as the Continuum Interpolation Band Ratio (CIBR) method [6-10] and as Atmospheric Precorrected Differential Absorption (APDA) method [11].

CIBR PW Retrieval

The CIBR method of CWV retrieval is based on the *CIBR* index defined by the equation

$$CIBR = \frac{F}{aE + bG} \tag{1}$$

where F is a satellite observed radiance in the channel within a water vapor absorption band, and E and G are radiances in nearby reference channels located on each side of the absorption band F (Fig. 1). The weighting coefficients, a and b, determine the linear combination of the two reference channels (E and G) used. These coefficients are usually weighted by the distance between the absorbing and the reference channels:

$$a = \frac{l_G - l_F}{l_G - l_E} \tag{2}$$

$$b = \frac{l_F - l_E}{l_G - l_E} \tag{3}$$

where l_E, l_F and l_G are the center wavelengths of the E, F and G channels.

DA and NW Methods

The CWV indices (*DA* and *N/W*) in the differential absorption and the narrow and wide methods are given by the ratio of appropriate radiances as

$$DA = \frac{F}{E} \tag{4}$$

and

$$NW = \frac{N}{W} \tag{5}$$

The MTI CIBR algorithm uses a broad absorption band (MTI band F) centered near the maximum of water vapor strong absorption band, and two reference bands (E and G) just outside the water vapor absorption (Fig. 1). MODIS uses three channels (MODIS channels17, 18 and 19) within water vapor absorption bands and two reference channels outside water vapor absorption bands [12].

5. ERROR ANALYSIS

The main sources of errors in the satellite retrieval can be divided into two groups with respect to their origin; errors of retrieval due to the environmental factors (e.g. not precisely known atmospheric temperature profiles, aerosol loading, greenhouse gases concentration, surface reflectivity) that differ from the assumed; and errors due to the calibration errors. The calibration sources of retrieval error include errors in pixel registration, radiometric calibration, and spectral registration. Contribution from individual sources to the total error of retrieval depends on whether errors within and in between individual channels are correlated or not. Correlated errors may partially cancel out while uncorrelated errors will generally add up to produce a larger total error. The uncertainties in environmental parameters are expected to produce a random kind of error (unless a major mistake is made in estimating values of various environmental variables), while calibration errors may lead to systematic errors in the retrieved quantities.

The individual channel radiances *E, F* and *G* have errors *DE, DF* and *DG* caused by the errors in the used atmospheric model and calibration. From Eq. (1) the relative error of the *CIBR* index can be written in the form

$$\frac{\Delta CIBR}{CIBR} = \frac{\Delta F}{F} - \left(\frac{\Delta E}{E}\frac{aE}{aE+bG} + \frac{\Delta G}{G}\frac{bG}{aE+bG}\right) + (\Delta)^2 \qquad (6)$$

where $(\Delta)^2$ stands for higher order terms in *DE, DF* and *DG*.

The calibration error in each channel can be approximated by a sum of three terms

$$\Delta L = \Delta L_{BC} + \Delta L_{BW} + \Delta L_{RAD} + \Delta L_{ENV} \qquad (7)$$

where *L* is radiance in a considered channel (E, F or G). The first three terms on the right hand side of (7) are due to calibration errors in the band center, DL_{BC}, band width, DL_{BW} and radiometric calibration, DL_{RAD} . The last term, DL_{ENV}, is due to uncertainty in environmental parameters, like atmospheric temperature and humidity profiles, atmospheric aerosol loading and spectral dependence of surface reflectivity.

The total first order relative error in the CIBR index, *DCIBR/CIBR*, can be written in the form

$$\frac{\Delta CIBR}{CIBR} = \frac{\Delta CIBR_{BC}}{CIBR} + \frac{\Delta CIBR_{BW}}{CIBR} + \frac{\Delta CIBR_{RAD}}{CIBR} + \frac{\Delta CIBR_{ENV}}{CIBR} \qquad (8)$$

where

$$\frac{\Delta CIBR_{BC}}{CIBR} = \frac{\Delta F_{BC}}{F} - \left(\frac{\Delta E_{BC}}{E}\frac{aE}{aE+bG} + \frac{\Delta G_{BC}}{G}\frac{bG}{aE+bG}\right) \tag{9}$$

Similar expressions can be written for other terms on the right hand side of Eq. (8).

Relative errors for the DA and NW methods can be written as

$$\frac{\Delta DA}{DA} = \frac{\Delta F}{F} - \frac{\Delta E}{E} + (\Delta)^2 \tag{10}$$

and

$$\frac{\Delta (NW)}{NW} = \frac{\Delta N}{N} - \frac{\Delta W}{W} + (\Delta)^2 \tag{11}$$

These errors can be again written as a sum of individual terms (similarly to Eq. 9) originating from the spectral band center, bandwidth, radiometric calibration and environmental errors.

The three-channel CIBR method, does not lead to a larger error than the two-channel DA or the NW method. This is easiest to see in the case when relative errors in reference channels E and G are approximately equal $DE/E = DG/G$. The CIBR index relative error as given by Eq. (6) is then reduced to

$$\frac{\Delta CIBR}{CIBR} = \frac{\Delta F}{F} - \frac{\Delta E}{E} \tag{12}$$

which is identical to Eqs. (10) and (11) for a relative error of a two-channel DA or NW method.

6. CALIBRATION ERRORS

Calibration errors include the errors in spectral band positions and widths, and in their radiometric calibration. The assumed shape of the spectral response function is a top-hat, e.g. constant within the band (Table 1) and zero outside.

Band positions

As a function of the band center position, the radiances in both reference channels, E and G, follow the basic radiance wavelength dependence as given by the solar radiation, decreasing towards the longer wavelength. The radiance change in the reference channels E and G is within 0.5% for shifts of channels' centers up to 1nm and within 1% for displacements up to 3nm (numerical calculations were done using the solar zenith angle of 30^o, satellite viewing angle of 0^o, rural aerosol with 23 km visibility and surafe albedo of 0.3). There is only a weak dependence of the radiance in these bands on the total amount of CWV.

The radiance of the broad absorbing channel F centered at 940 nm shows a stronger dependence on the channel position. In addition, this dependence also varies with the total amount of CWV. The relative radiance error is within 2% for the shifts up to 2nm. The band center displacement in either direction leads generally to higher values of the band F radiance (Fig. 2). Thus any error in the exact spectral position of the water vapor absorbing band (towards the shorter or longer wavelengths) will lead to a systematic underestimate of the CWV. The radiance error due to the spectral shift of channel F is generally larger than radiance errors in reference channels E or G.

Band Width

The increasing spectral width of any band leads to almost a linear increase of the radiance at satellite level. The radiance in the absorbing channel F depends also on the amount of CWV**.** The 0.5 nm increase in the bandwidth leads to about 2% increase in the E channel, about 1% increase in G channel, and between 1 and 2.5% increase in band F (depending on the CWV amount).

The original errors in bands positions and bandwidths, as determined by pre-flight laboratory measurements, are relatively small, within 0.5 nm. Larger shifts may occur during the flight due to various environmental effects and instrumental changes. We assume that the in-flight changes would affect all bands in a similar manner and therefore that the errors in individual bands would be mutually correlated. If the bandwidth error is the same for all three channels, the errors have tendency to cancel out and the resulting error due to bandwidth changes (Fig. 3) in the *CIBR* index is relatively small (within 0.5% for the amount of CWV<3 cm and within 1% for the CWV up to 6 cm with the bandwidth change of up to 0.5 nm).

Radiometric calibration

A radiometric calibration error occurs when the digital number *DN* of a given channel is transformed to the radiance (in watts per unit area per unit solid angle). The laboratory pre-flight calibration uses a set of pre-calibrated lamps. The expected radiometric error of individual channels is between 1 and 3%. The MTI reference channels E and G are outside the water vapor absorption band and the radiances are comparable in magnitude. A single light source can be used for calibration of these two channels. At high CWV values, the radiance in the F channel will be significantly reduced and a lower intensity source has to be used for calibration. Consequently, the radiometric calibration errors between the reference channels (E and G) and the absorption channel F are more likely to be uncorrelated.

7. UNCERTAINTIES IN ATMOSPHERIC VARIABLES

The MTI retrieval of the CWV uses the MODTRAN radiative transfer model calculations with the MODTRAN specified atmospheric profile and aerosol. To determine how the choice of these parameters affects the accuracy of the CWV retrieval, we have calculated the CIBR index for given amount of CWV and different aerosols and atmospheric profiles.

Atmospheric temperature and humidity profiles

We find that the CIBR index is not a sensitive function of the chosen atmospheric temperature and humidity profile. Even with the choice of an inappropriate atmosphere (e.g. using the tropical instead of midlatitude winter atmospheric profile) the maximum difference between obtained CIBR values are generally within 1% from each other (Fig. 4). Only tropical model atmosphere can hold realistically the CWV amount larger than

4.5 g/cm^2. Therefore comparison between two or more MODTRAN model atmospheres is not possible for CWV>4.5 g/cm^2.

Spectral dependence of surface reflectivity

The CIBR and the APDA methods of CWV retrieval eliminate partially the errors due to spectral dependence of the surface albedo [13]. In the case of soils containing a large amount of iron oxides the compensation between the bands is incomplete. To avoid a possible error in the CWV retrieval due to spectral absorption of soils, we look first for pixels covered by vegetation and proceed with the CWV retrieval using these selected pixels.

Aerosols

Atmospheric aerosol has a strong effect on the deduced amount of CWV. In our model calculations we have used the standard MODTRAN rural aerosol with the boundary layer visibility of 5, 23 and 50 km (with a multiple scattering in two stream approximation). A real aerosol just in between the standard MODTRAN visibility range from 5 to 23 km or between 23 and 50 km will introduce an error in the CIBR index up to 6% (Fig. 5). According to our analysis, the uncertainty in atmospheric aerosol seems to be the largest possible source of errors in the CWV retrieval.

The error in the CIBR index propagates into the error in the CWV retrieval. The relation between the CIBR and the CWV error depends on the amount of the CWV. Assuming the CIBR index error of 5%, the maximum error in CWV amount, almost 0.6 cm, occurs around CWV amount of 4 cm (Fig. 6). This translates into the CWV error of about 15%.

8. MTI COLUMNAR WATER VAPOR RETRIEVAL - VALIDATION

To evaluate the accuracy of the MTI water vapor retrieval, we compared the satellite derived columnar water vapor amount with “ground truth” measurements. For this purpose we used AERONET (AErosol RObotic NETwork) [14] total columnar water vapor measurements at the Oklahoma DOE ARM (Atmospheric Radiation Measurement) and NASA Stennis Space Center sites. The assumed accuracy of AERONET measurement is about $\pm$ 10% [15]. We have 51 MTI clear sky or partially cloudy images available for the validation.

Combining the Oklahoma DOE ARM and the Stennis site AERONET columnar water vapor data (Fig. 7) for validation of the MTI CWV retrieval leads to the RMS error of the retrieval of 14.2% (using the CIBR code). A large percentage error usually occurs for cases of low water vapor amounts, even when the absolute error is quite small. Considering only the cases with the total amount of CWV over 1 g/cm^2, the RMS error of the MTI CWV retrieval using the CIBR algorithm is around 12.0%. We have found no significant differences in accuracy between the CIBR and the APDA methods. The comparison was performed over vegetation (which appears bright in the near infrared). Over low ground reflectance regions, the APDA is expected to provide more accurate retrievals than the CIBR method [13].

9. A NOTE ON NIGHTTIME COLUMNAR WATER VAPOR RETRIEVAL

Most satellite based water vapor monitoring has been limited to the daytime hours. This is due to the fact that many of the operational water vapor products use reflected near infrared solar radiation for CWV retrieval. Additional information concerning the nighttime water vapor amount and its variability would contribute to our understanding of the hydrological cycle and climate.

Several research groups have developed methods for columnar water vapor estimates using the wavelengths between 10 and 13 μm. Specifically channels 4 (10.3 to 11.3 μm) and 5 (11.5 to 12.5 μm) of the NOAA AVHRR (Advanced Very High Resolution Radiometer) sensor have been explored for this purpose. The methods include the split-window temperature difference technique and its modifications [17], ratio of variances and the covariance-variance technique [18]. These approaches were only partially successful. Jedlovec [19] found correlation between the retrieved and the measured total water vapor to be below 0.1. Barton and Prata [20] applied the covariance-variance technique using the AVHRR channels 4 and 5 and reported no correlation with independent water vapor measurements. Czajkowski et al. [21] report only very low correlations between the near-surface water vapor measurements and four different methods of estimate using the AVHRR channels 4 and 5 radiances.

To understand these results we model the top of the atmosphere outgoing radiances using the MODTRAN 4.0 radiative transfer code with the standard mid-latitude atmospheric profile. The total radiance received by a satellite sensor comes from two basic sources: from the surface (surface emission) and from the atmosphere (path emission). The detector cannot discriminate between radiation emitted by the surface and radiation emitted by the atmosphere. The total radiance, within 10 to 13 μm region, seen by the sensor (the sum of the surface and the path radiance) shows a relatively weak dependence on the CWV (Fig. 8). At the surface temperature of 303K, the top of the atmosphere outgoing radiance changes by about 20% with the change of CVW from 0.1 to 4 cm (Fig. 9a). This change is reduced to about 6% for the surface temperature of 293K (Fig. 9b) and to about 3% for the surface temperature of 283K. At mid-latitudes at nighttime the average temperature is often below 293K. Considering a low sensitivity of the top of the atmosphere radiances to the CWV amount (at surface temperature of 293K and lower), it seems that any method using the spectral bands within the 10 to 13 μm region cannot lead to an accurate estimates of total water vapor amounts.

In the middle infrared region, between 4.5 to 5.5 μm, the effect of the total water vapor amount on the outgoing top of the atmosphere radiances is considerably stronger (Fig. 9) than in the 8 to 13 μm region. The nighttime CWV retrieval using the mid-infrared region should be more accurate than the retrieval in the 10 to 13 μm region. This should be taken into the consideration in planning and developing future satellite instruments designated to retrieve the CWV amounts at nighttime.

10. SUMMARY AND DISCUSSION

The largest error in the CWV retrieval is caused by uncertainty in aerosol optical depth and by calibration errors of the water vapor absorbing band, the band F in the case of the MTI. Thus the satellite sensors that can simultaneously retrieve the aerosol optical depth and use this measurement as an input into the CWV retrieval may achieve a higher accuracy in the CWV retrieval. Published model-based estimate of the MODIS CWV retrieval using the CIBR method [12] suggests 13% error using the standard aerosol models, and 7% error if additional inputs including aerosol optical thickness are provided. The achieved RMS error of the MTI instrument (about 14%) is in a reasonable agreement with results of theoretical analysis [12]. The obtained accuracy can be further improved by using simultaneously retrieved information concerning aerosol optical depth [22].

The nighttime CWV retrieval remains to be an unsolved problem. Contradictory claims in publish literature can be partially understood by a low sensitivity of the long infrared radiances to the CWV at lower surface and atmospheric temperature. The mid-infrared region seems to be more suitable for the nighttime water vapor retrieval.

Acknowledgment

We thank W. Atkins, S. Bender, W. Clodius, and A. Rodger for helpful discussions.

Table 1: List of spectral bands of the DOE MTI. Bands E, F, and G are used for the CWV retrieval using the CIBR or APDA algorithm.

MTI Band	Central Wavelength (μm)	Band Width (μm)
A	0.484	0.057
B	0.558	0.066
C	0.650	0.050
D	0.810	0.086
E	0.874	0.025
F	0.940	0.056
G	1.015	0.048
H	1.376	0.027
I	1.646	0.193
O	2.224	0.271
J	3.787	0.565
K	4.957	0.174
L	8.225	0.334
M	8.656	0.379
N	10.471	0.456

References

1. Peixoto, J. P., and Oort, A. H., 1992, *Physics of Climate*, American Institute of Physics, New York.
2. Goody, R. M., and Yung, Y. L., 1989, *Atmospheric Radiation*, Oxford University Press, New York.
3. P. G. Weber, C. C. Borel, W. B. Clodius, B. J. Cooke, and B. W. Smith, 1999, *Proc. SPIE Conference on Infrared Imaging Systems: Design, Analysis, Modeling, and Testing*, SPIE Vol. 3701, paper 3701-13.
4. Bennartz, R, and Fischer, J., 2001, *Remote Sens. Environ*. 78, 274.
5. Frouin, R., Deschamps, P-Y., and Lacomte, P., 1989, *J. Appl. Meteorol*. 29, 448.
6. Gao, B. C., and Goetz, A. F. H., 1990, *J. Geophys. Res*. 95, 3549-3564.
7. Bruegge, C. T., Conel, J. E., Green, R. O., Margolis, J. S., Holm, R. G. and Toon, G., 1992, *J. Geophys. Res.*, 97, 18759.
8. Kaufman, Y. J., and Gao, B. C., 1992, *IEEE Trans. Geosci. Remote Sens*. 30, 871.
9. Carrere, V., Conel, J. E., 1993, *Remote Sens. Environ.* 44, 179.
10. Tahl, S., and Schonermark, M. v., 1998, *Int. J. Remote Sens*. 19, 3223.
11. Schlapfer, D., Borel, C. C., Keller, J., and Itten, K. I.,1998, *Remote Sens. Environ*. 65, 353.
12. King, M. D., Kaufman, Y. J., Menzel, W. P., and Tanre, R., 1992, *IEEE Trans. Geosci. Remote Sens*. 30, 2.
13. Borel, C. C., Clodius, W. B, and Johnson, J., 1996, *SPIE* Vol.2758, 218.
14. Holben, B. N., Eck, T. F., Slutsker, I., Tanre, D., Buis J. B., Setzer,A., Vermote, E., Reagan, J. A., Kaufman, Y. J., Nakajima, T., Lavenu, F., Jankowiak, I., and Smirnov, A., 1998, *Remote Sens. Environ.*, 66, 1.
15. Eck, T.,and Holben, B., 2003, private communication.
16. Chylek, P., Borel. C., Clodius, W., Pope, P., and Rodger, A., 2003, *IEEE Trans. Geosci. Remote Sens.*, submitted for publication.
17. Dalu, G., 1986, *Int. J. Remote Sens*. 7: 1089
18. Ottle, C., and Francois, C., 1999, *Remote Sens. Environ.*, 69, 84.
19. Jedlovec, G. J., 1990, *J. Appl. Meteor.*, 29, 863.
20. Barton, I. J., and Prata, A. J., 1999, *Remote Sens. Environ.*, 69, 76.
21. Czajkowski, K. P., Goward, S. N., Shirey, D. and Walz, A., 2002, *Remote Sens. Environ.*, 79, 253.
22. Chylek, P., Henderson, B., and Mishchenko, M., 2003, *Geophys. Res. Lett.*, in press.

Figure Captions:

Fig. 1: Top of the atmosphere outgoing radiances (averaged over 50 cm^{-1}) within the 850 to 1050 nm region. The radiances were obtained using the MODTRAN 4.0 code in a multiple scattering two-stream mode for the mid-latitude summer atmosphere with CWV amount of 3 cm, with stratospheric background aerosol and tropospheric rural aerosol of 23km boundary layer visibility. The surface albedo 0.3, solar zenith angle 30^o and the satellite zenith angle 0^o(a nadir look) are used. Positions and widths of the MTI bands used for CWV retrieval are indicated.

Fig. 2: Error in the MTI F band radiance due to an error in band center position.

Fig. 3: Error in the MTI F band radiance due to an error in the band width.

Fig. 4: Error in the MTI E, F and G band radiances and the CIBR index due to use of different standard atmospheric profiles (tropical, midlatitude summer, midlatitude winter, subarctic summer, subacrtic winter) in the MODTRAN radiative transfer code.

Fig. 5: The value of the deduced CIBR index depends on the aerosol model used (rural aerosol with the boundary layer visibility of 50, 23 and 5 km) in the MODTRAN code.

Fig. 6: The error in the CWV retrieval, for CIBR index errors of 1, 3 and 5%, as a function of the CWV.

Fig. 7: The validation of the MTI CIBR CWV retrieval with respect to the AERONET data suggests the RMS error of 14% (after Chylek et al. [21]).

Fig. 8: The top of the atmosphere outgoing radiances in the 8 to 13 μm atmospheric window (averaged over 30 cm^{-1}) for indicated amounts of CWV and surface temperature of 303K (8a) and 293K (8b). Calculations are done using the MODTRAN code with the standard mid-latitude summer atmosphere assuming emissivity $\varepsilon=1$.

Fig. 9: The top of the atmosphere outgoing radiances in the 3.5 to 5.5 μm atmospheric window (averaged over 30 cm^{-1}) for indicated amounts of CWV and surface temperature of 303K (9a) and 293K (9b). Calculations are done using the MODTRAN code with the standard mid-latitude summer atmosphere assuming emissivity $\varepsilon=1$.

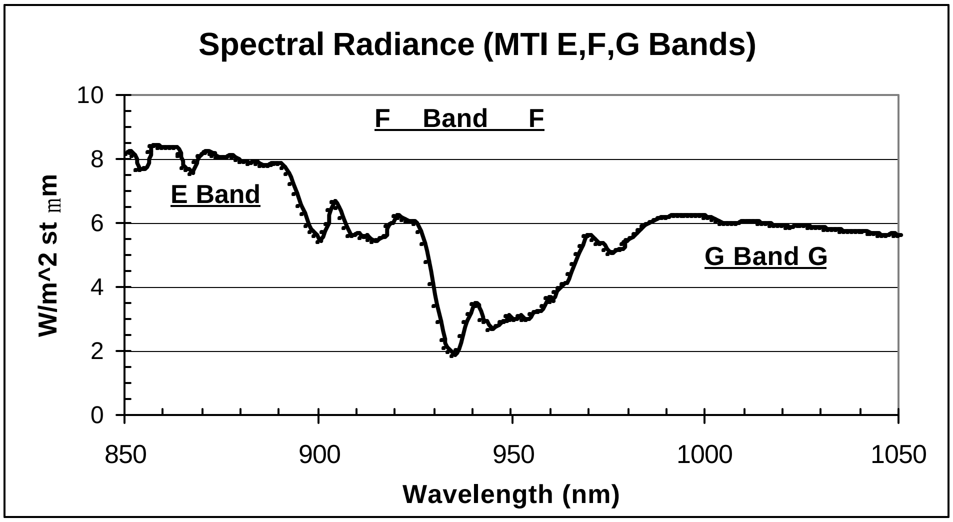
Spectral Radiance (MTI E,F,G Bands)
F Band F
E Band
G Band G
W/m^2 st mm
10
8
6
4
2
0
850
900
950
1000
1050
Wavelength (nm)

Fig. 1

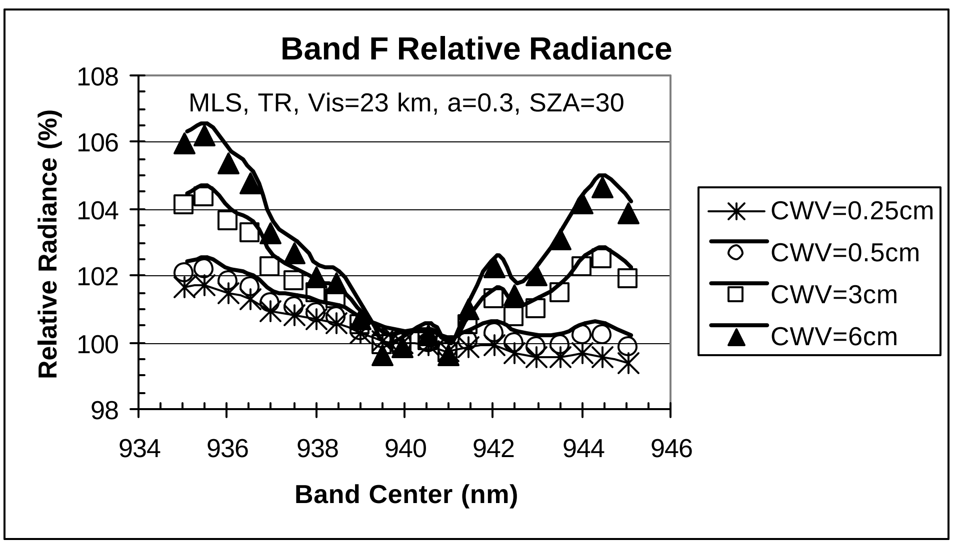
Band F Relative Radiance
MLS, TR, Vis=23 km, a=0.3, SZA=30
Relative Radiance (%)
108
106
104
102
100
98
934
936
938
940
942
944
946
Band Center (nm)
CWV=0.25cm
CWV=0.5cm
CWV=3cm
CWV=6cm

Fig. 2

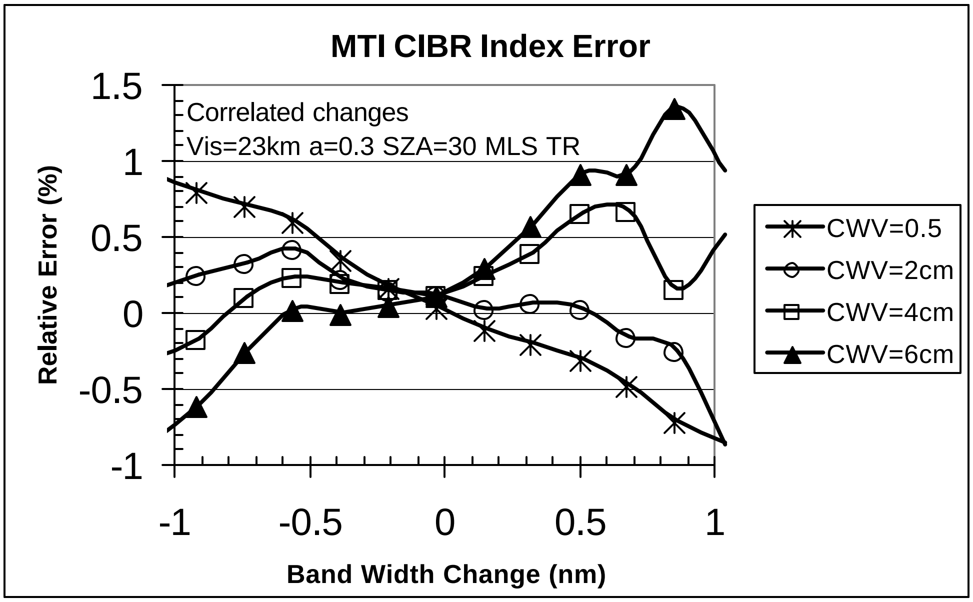
MTI CIBR Index Error
Correlated changes
Vis=23km a=0.3 SZA=30 MLS TR
1.5
1
0.5
0
-0.5
-1
Relative Error (%)
-1
-0.5
0
0.5
1
Band Width Change (nm)
CWV=0.5
CWV=2cm
CWV=4cm
CWV=6cm

Fig. 3

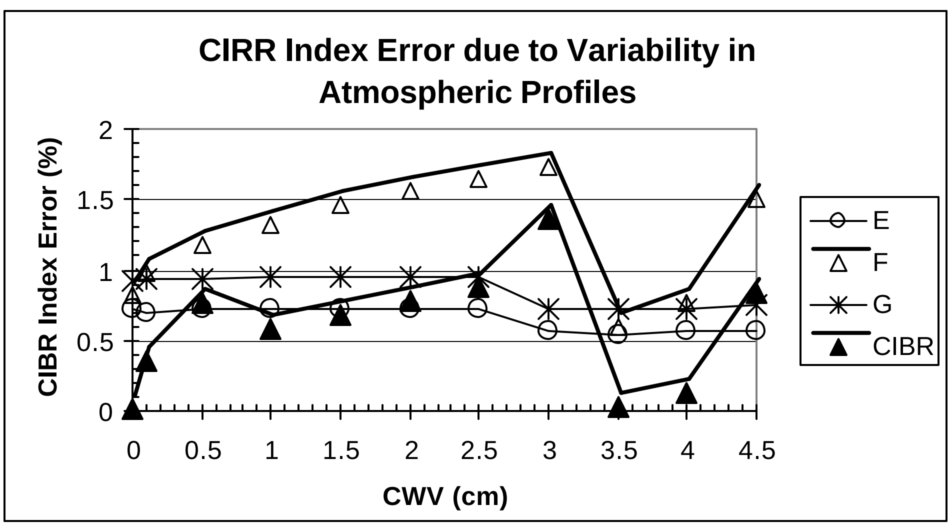
CIRR Index Error due to Variability in Atmospheric Profiles
2
1.5
1
0.5
0
CIBR Index Error (%)
0
0.5
1
1.5
2
2.5
3
3.5
4
4.5
CWV (cm)
E
F
G
CIBR

Fig. 4

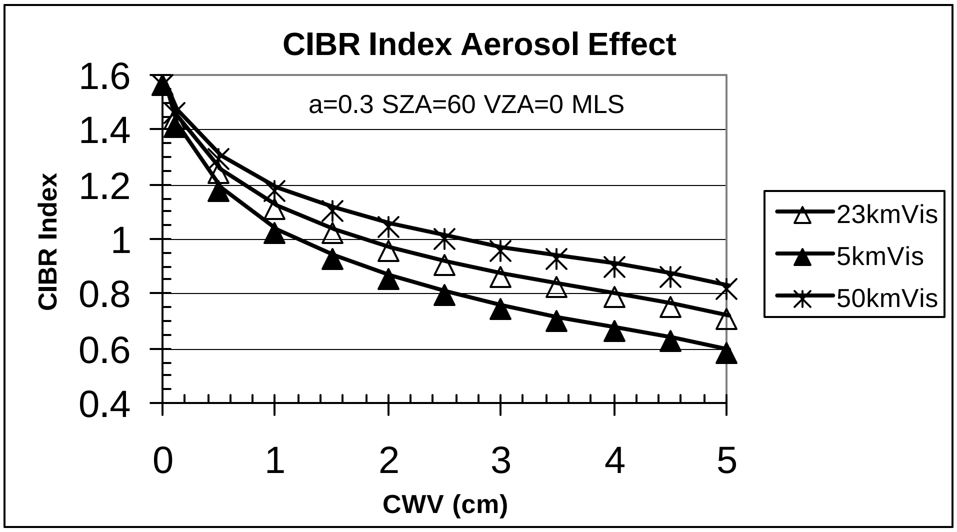

CIBR Index Aerosol Effect
a=0.3 SZA=60 VZA=0 MLS
CIBR Index
1.6
1.4
1.2
1
0.8
0.6
0.4
0
1
2
3
4
5
CWV (cm)
23kmVis
5kmVis
50kmVis

Fig. 5

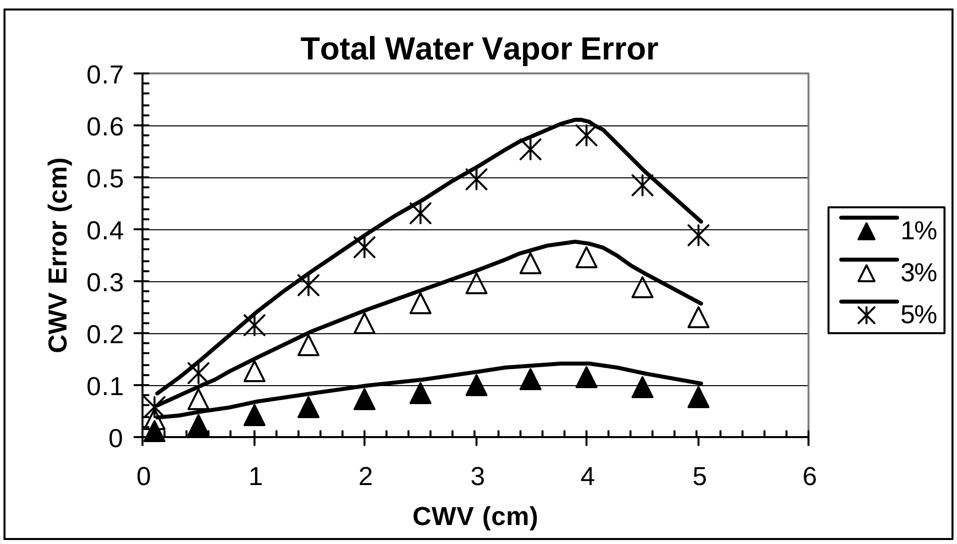

Total Water Vapor Error
CWV Error (cm)
0.7
0.6
0.5
0.4
0.3
0.2
0.1
0
0
1
2
3
4
5
6
CWV (cm)
1%
3%
5%

Fig. 6

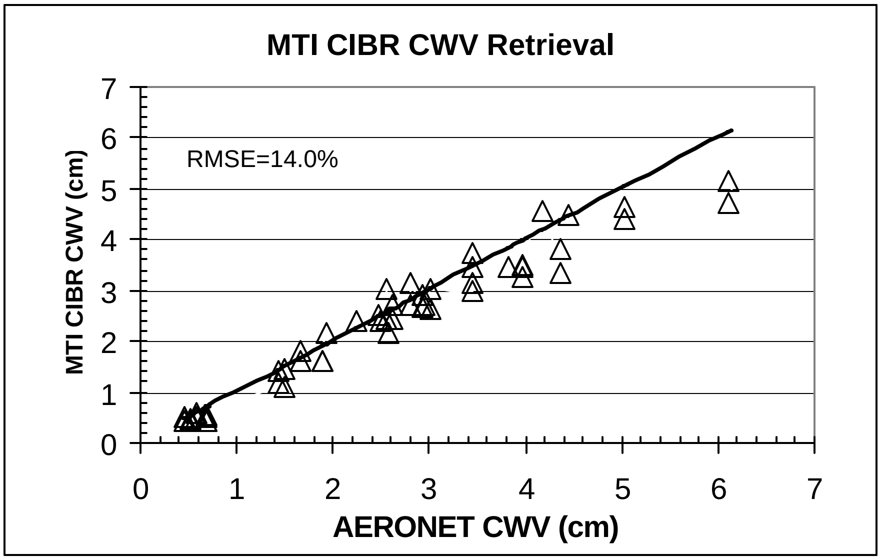
MTI CIBR CWV Retrieval
RMSE=14.0%
MTI CIBR CWV (cm)
AERONET CWV (cm)
0
1
2
3
4
5
6
7

Fig. 7

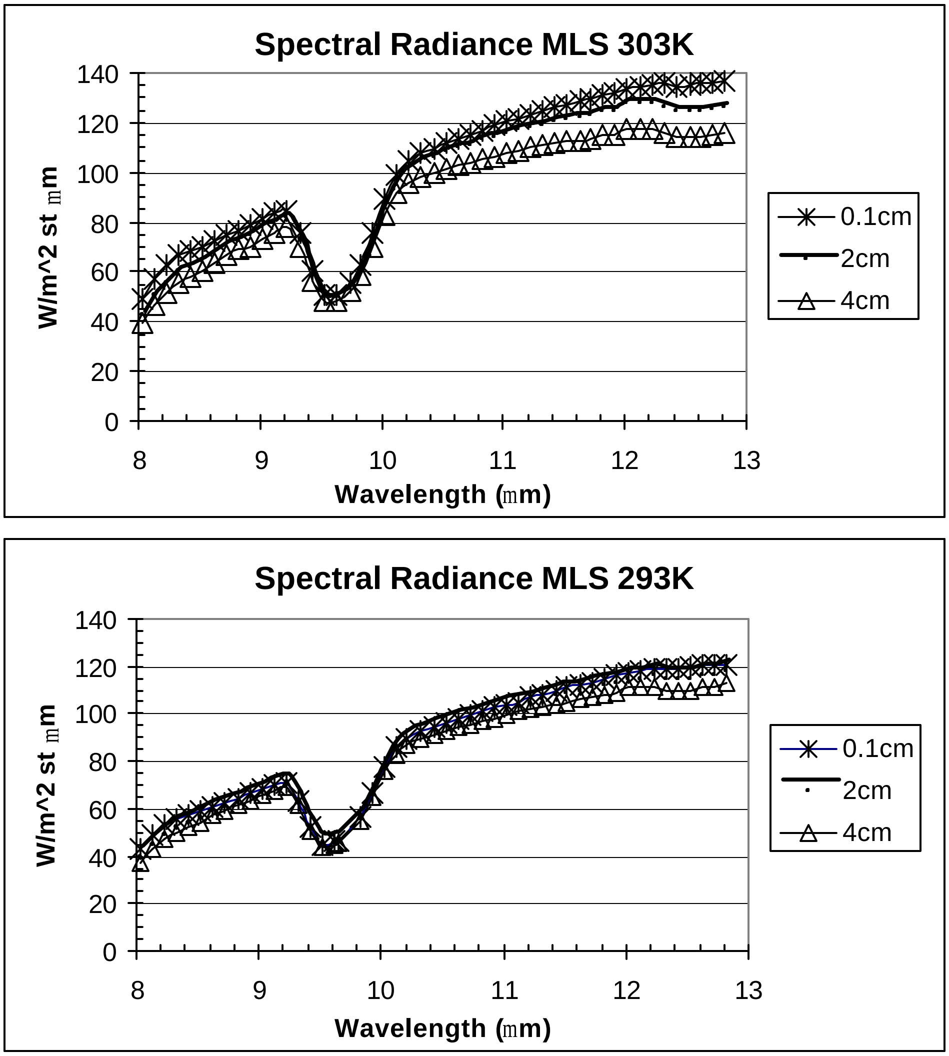
Spectral Radiance MLS 303K
W/m^2 st ㎜m
Wavelength (㎜m)
0.1cm
2cm
4cm
Spectral Radiance MLS 293K
W/m^2 st ㎜m
Wavelength (㎜m)
0.1cm
2cm
4cm

Fig. 8

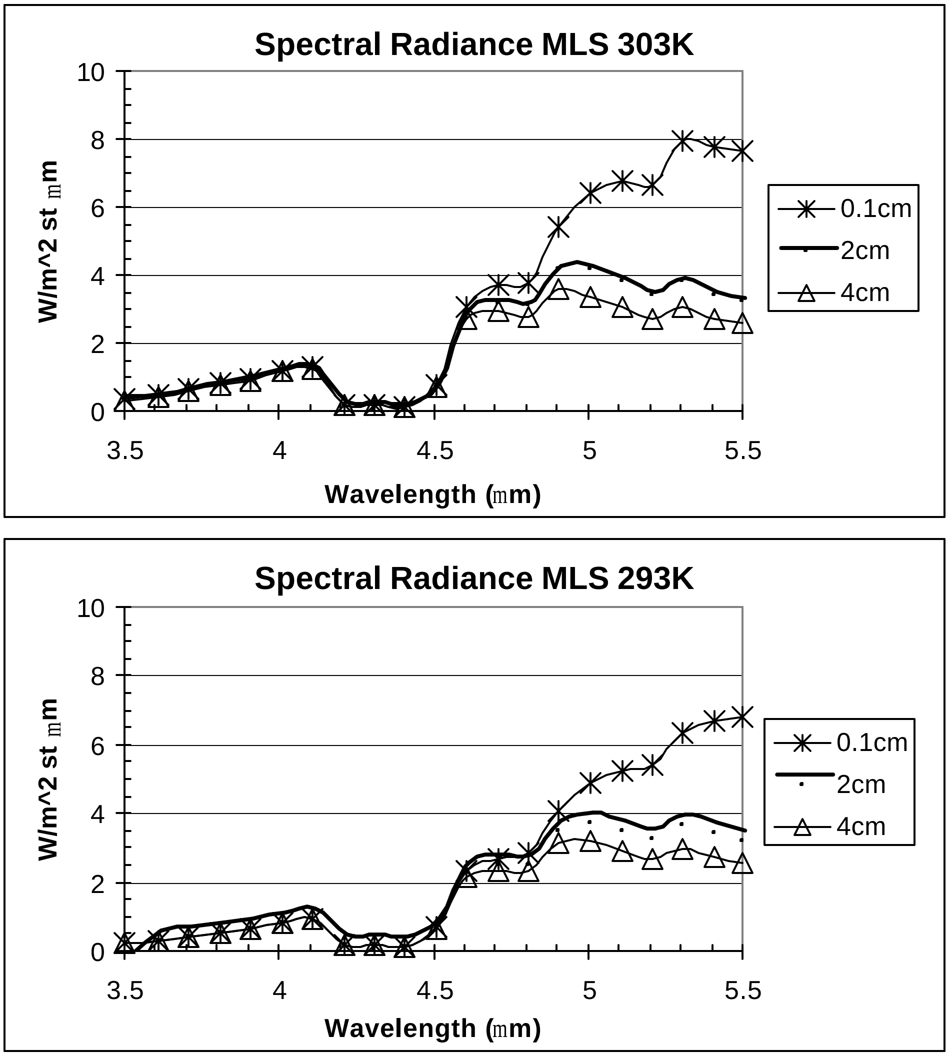
Spectral Radiance MLS 303K
W/m^2 st µm
Wavelength (µm)
0.1cm
2cm
4cm
10
8
6
4
2
0
3.5
4
4.5
5
5.5
Spectral Radiance MLS 293K
W/m^2 st µm
Wavelength (µm)
0.1cm
2cm
4cm
10
8
6
4
2
0
3.5
4
4.5
5
5.5

Fig. 9